Available online at www.sciencedirect.com
SCIENCE DIRECT®
Pergamon
Cement and Concrete Research 34 (2004) 631–640
CEMENT AND CONCRETE RESEARCH

Ultrasonic in-situ monitoring of setting process of high-performance concrete

H.K. Lee[a,*], K.M. Lee[a], Y.H. Kim[b], H. Yim[c], D.B. Bae[d]

[a]*Department of Civil and Environmental Engineering, Sungkyunkwan University, 300 Chunchun-dong, Jangan-gu, Suwon, Kyunggi-do 440-746, South Korea*
[b]*School of Mechanical Engineering, Sungkyunkwan University, Suwon, South Korea*
[c]*Department of Mechanical Engineering, Hongik University, Seoul, South Korea*
[d]*Department of Civil and Environmental Engineering, Kookmin University, Seoul, South Korea*

Received 30 May 2002; accepted 6 October 2003

Abstract

The present standard test for the setting times of concrete is the penetration resistance test specified by ASTM C403. This test, while good for standard concrete mixtures, may not be appropriate for high-performance concrete (HPC) because of the high viscosity of the mortar. To address this issue, the ultrasonic pulse velocities (UPV) were measured using an ultrasonic monitoring system during the first 24 h of age for mortar and concrete specimens having various water-to-cementitious materials (w/cm) ratios and with and without fly ash (FA). Various characteristics observed from the measured UPV agreed with the previous theory of cement hydration, which describes the mixture as viscous suspension transforming into saturated porous solid phase. It was also found that the development of UPV in concretes, particularly without FA, was faster than that of mortars with the same w/cm. The values of concrete UPV corresponding to the initial and final setting (ASTM C403) did not show a trend consistent with those of mortar UPV. Two alternative criteria were applied to determine the setting characteristics from the UPV evolution curves. They were found to better represent the microstructural changes than the penetration method, as suggested by the consistent trend with decreasing w/cm among various mortars and concretes. Thus, the potential use of these alternative methods is suggested by specifying, at each w/cm, general target UPVs that are valid for both mortar and concrete with or without FA. It was concluded that the methods and monitoring device used in this research were useful for the in-situ monitoring of the setting of concrete, particularly in HPC.

Keywords: High-performance concrete; Setting time; Penetration resistance; Ultrasonic pulse velocity; Fresh concrete; Mortar; Fly ash

1. Introduction

Accurate field measurements of early-age properties of concrete, such as the setting time and strength, are crucial to operations scheduling and in-situ quality control of concrete. Recently, the use of high-performance concrete (HPC) has increased dramatically; however, few studies have been conducted on the early-age properties of HPC. Because of the low water-to-cementitious materials (w/cm) ratio and the use of various chemical and mineral admixtures, these properties may be quite different from those of ordinary concrete and more detailed study is called for.

According to ASTM C403 [1], the initial and final setting of concrete are determined when the penetration resistance of a sieved mortar sample reaches 3.5 and 27.6 MPa, respectively. These values of penetration resistance correspond to two particular practical points, loosely defined as the limit of handling and the beginning of mechanical strength development, respectively; therefore, these resistance values, fixed regardless of the concrete composition, cannot be associated with the characteristic physicochemical and microstructural changes of concrete [2]. One disadvantage of the penetration resistance method is that its accuracy depends largely on the skill and experience of the person performing the test. Moreover, the method may not even be applicable to HPC because a sieved mortar sample can hardly be obtained because of its high viscosity.

* Corresponding author. Tel.: +82-31-290-7516; fax: +82-31-290-7549.
E-mail address: leekm79@skku.edu (K.K. Lee).

0008-8846/$ – see front matter © 2004 Elsevier Ltd. All rights reserved.
doi:10.1016/j.cemconres.2003.10.012

Pessiki and Carino [3] used the impact-echo method to compare the measured wave velocity with the measured penetration resistance. They defined the setting of concrete as when the wave velocity begins to increase or when a specified wave velocity is reached. This method, however, may not be practical for early-age concrete because concrete is in the form of viscous suspension at its very early age and thus may be hard to "impact" on.

An alternative method for determining the setting behavior of concrete is the use of ultrasonic waves. Keating et al. [4,5] observed that the velocity of longitudinal ultrasonic wave in cement slurries exhibited three regimes as time elapses after mixing: an initially constant regime, a rapidly increasing regime and a much slowly increasing or almost constant regime. Similar patterns of evolution of longitudinal ultrasonic pulse velocity (UPV) in mortars and concretes have been observed by many other researchers [6–14]. Most of them compared the evolution of the longitudinal wave velocity with that of other parameters and concluded that the changes in the longitudinal wave velocity are related to the hydration of cement. For example, Chotard et al. [8] and Smith et al. [9] found that the longitudinal wave velocity is sensitive to the massive formation of hydrates and that the duration of its sharp increase corresponds to the cement stiffening process. It is also noteworthy that the air content in the mortar was observed by researchers [4,5,12] to have drastic effects on reducing the velocity of longitudinal ultrasonic waves because it causes severe attenuation due to wave scattering.

Sayers and Grenfell [12] compared their experimental results of longitudinal and shear wave velocities with the theory developed by Biot [15] and concluded that during the hydration of cement the solid phase becomes highly connected (an example of percolation transition) and the material transforms from a viscous suspension of irregularly shaped cement particles into a porous elastic solid with nonvanishing elastic moduli. The work by D'Angelo et al. [13] about hydrating cement slurries led to the conclusion that the onset of shear wave propagation is a clear indicator of the percolation transition, which may not so clearly be identified from the longitudinal wave behavior. Boumiz et al. [14] conducted ultrasonic, calorimetric and conductometric studies on early-age cement pastes and mortars and concluded that the percolation of the solid phase causes dramatic changes in the ultrasonic wave behavior. Recently, the shear wave reflection coefficient at the interface between the specimen and the container has been studied [16–18]. This method is particularly useful for in situ cases where only one side of the test specimen is accessible.

Although it has been mentioned in other works [9,12,13,16,18], the "percolation" of solid phases in hydrating cements has been understood more thoroughly via simulation studies using a three-dimensional model [19–21]. The term percolation here is defined to be the establishment of a path solely of a phase from one end of the specimen to the other end. These researchers, as many others cited above, described the hydrating cement or mortar as viscous suspension changing to water-saturated porous solid.

Several suggestions have been made for the identification of characteristic points of cement hydration from the evolution of parameters related to ultrasonic waves [5,7–9,16,21]. For instance, Kakuta and Kojima [6] defined the setting time as the instant when the increasing rate of dynamic shear modulus reaches its maximum. Chotard et al. [8], Smith et al. [9] and Garnier et al. [10] expected the two kinks, typically observed from the evolution curve of longitudinal wave velocity, to be related to the characteristic points of the setting process. Rapoport et al. [16] considered two bends (labeled A_S and B_S) in the shear reflection coefficient curve and supposed them to be related to the percolation of cement grains and the depercolation of the water phase, respectively. Furthermore, Bentz et al. [20] defined the set point rigorously as the point of solids percolation.

In spite of the great number of related previous studies including those mentioned above, pertinent experimental studies for HPC are scarce. In the present work, HPC specimens having various low w/cm (with or without fly ash [FA]) were prepared and their longitudinal UPV were measured as a function of the age using a monitoring system devised by Reinhardt et al. [11]. The evolution of characteristics of ultrasonic waves propagating through a setting mortar is examined. The development profiles of the UPVs of various specimens are closely investigated to study the effects of coarse aggregates, FA and w/cm. In addition, the UPVs corresponding to three setting criteria, including those based on the penetration resistance, for various specimens are obtained, and their tendency is studied and explained.

2. Experimental setup

2.1. Materials and mix proportions

Type I Portland cement and low-calcium FA produced in coal-fueled electric power stations in Korea were used as the cementitious materials. Their physical properties and chemical compositions are given in Table 1. The fine and coarse aggregates used were washed river sand with specific gravity of 2.51 and water absorption of 1.52% and crushed granite with specific gravity of 2.64 and fineness modulus of 6.88, respectively.

Table 1
Physical properties and chemical compositions of cement and FA

Materials	Physical properties		Chemical compositions (%)						
	Specific gravity	Blaine (cm^2/g)	SiO_2	Al_2O_3	Fe_2O_3	CaO	MgO	SO_3	LOI
Cement	3.15	3450	20.68	5.16	3.02	62.42	4.71	2.42	1.36
FA	2.27	3375	56.69	21.17	6.01	6.68	1.41	0.11	3.44

Table 2
Mix proportions of concrete per cubic meter

Mix no.	Water (kg)	Cement (kg)	FA (kg)	Fine aggregate (kg)	Coarse aggregate (kg)	AEWR (cm × wt.%)	HRWR (cm × wt.%)	w/cm
1	185	370	–	754	969	0.5	–	0.50
2	158	450	–	672	1061	–	1.5	0.35
3	155	500	–	626	1074	–	2.0	0.31
4	148	550	–	617	1060	–	2.4	0.27
5	185	296	74	744	956	0.5	–	0.50
6	158	360	90	661	1043	–	1.5	0.35
7	155	400	100	614	1054	–	2.0	0.31
8	148	440	110	605	1038	–	2.4	0.27

w/cm (cement + FA) ratio.
Mixes 1–4 = OPC series, Mixes 5–8 = FA series.

Table 2 shows the mix proportions of the eight concretes used in the experiments. The w/cm ranged from 0.27 to 0.50. Mixes 1–4 did not contain FA and were designated as the ordinary Portland cement (OPC) concrete series, whereas Mixes 5–8 contained FA of 20% weight of cementitious materials and were designated as the FA concrete series. The maximum size of coarse aggregate was 25 mm for normal-strength concrete (NSC) mixes (Mixes 1 and 5) and 20 mm for HPC mixes (Mixes 2–4 and 6–8). Mortar mixtures with the same w/cm and the same FA content as these concrete mixtures were also prepared for the penetration resistance tests.

Air-entraining water reducer (AEWR), as much as 0.5% weight of cementitious materials, was incorporated into NSC mixes, and a naphthalene sulfonate-based high-range water reducer (HRWR) was used to ensure the workability for the HPC mixes. To simulate actual applications in the field, concrete mixes having adequate workability were used.

2.2. Test equipment and procedure

An UPV monitoring system, which can measure the UPV at any desired intervals after casting, was constructed by following Reinhardt et al. [11]. As schematically shown in Fig. 1, the monitoring system consisted of two 40-mm-thick acrylic plates, a foam rubber container, a commercial UPV measurement device and two ultrasonic transducers with a center frequency of 54 kHz. Because the transducers were of longitudinal wave type, the UPV device measured the longitudinal wave velocity. Four bolts, shown in Fig. 1a and c, were fastened sufficiently to assure good contact between the specimen and the acrylic plates. Each acrylic plate had, at its midheight (see Fig. 1b), a circular hole of 51 mm diameter and 35 mm depth. A 50-mm-diameter transducer was fitted into the hole and pushed all the way to the bottom, with sufficient amount of couplant on its face. Fresh mortar or concrete was then poured in the container and compacted.

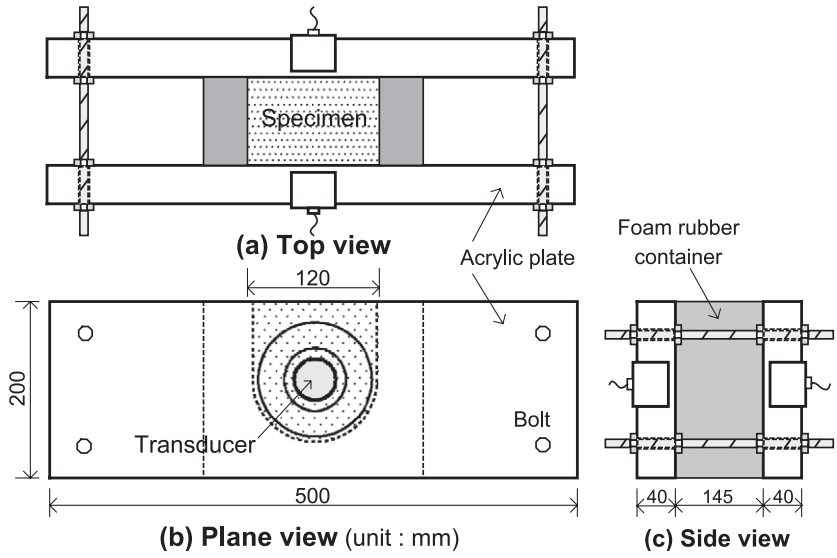

Fig. 1. Schematic diagram of monitoring system.

The UPV measurement started immediately after casting and continued for 24 h; yet, the results were recorded only at 30-min intervals because these intervals turned out to be sufficient to capture all important trends of the UPV development. The UPV (V_p) was calculated as follows:

$$V_p = L/t_p \quad (1)$$

where L is the length of the straight wave path through the specimen (i.e., 145 mm in this study) and t_p is the travel time of the ultrasonic pulse through L, excluding the travel time through the short acrylic paths in front of the transducer faces. Because the actual wave path may well be much longer than L at such early ages, the wave velocity computed by Eq. (1) should be regarded as the "average" or "apparent" wave velocity initially through the viscous suspension and then through the water-saturated porous solid medium. It is important to mention that no significant waves propagating through the foam rubber container wall were detected by the device because of high dissipation of the foam rubber.

To investigate the repeatability of measurement, t_p was measured thrice at each of several initial instants. The repeatedly measured t_p values were almost identical (i.e., they were within the resolution of time measurement, 0.2 μs). Therefore, only one measurement of t_p was taken at all other instants, and UPV was calculated using Eq. (1). Based on the resolution of time measurement, the accuracy of calculated UPV using Eq. (1) is to within 3 m/s.

3. Results and discussion

3.1. Properties of fresh and hardened concretes

Table 3 lists the values of slump and flow during the first hour after mixing and the initial air content of all fresh concrete mixtures. All mixtures exhibited high workability with respect to the slump and flow up to 1 h without noticeable segregation. Initial slumps of the NSC mixtures measured 190 mm while those of the HPC mixtures were 230 ± 20 mm. Because these high-performance mixtures exhibit low slump losses, they would be appropriate for use at actual construction sites. Table 3 also shows that the initial air content ranged from 1.6% to 5.0% as measured in accordance with ASTM C231.

Table 3
Properties of fresh concrete and setting times

Mix no.	Slump (cm)			Flow (cm)			Air content (%)
	Initial	30 min	60 min	Initial	30 min	60 min	Initial
1	19.0	18.0	15.0	41 × 40	36 × 35	30 × 31	5.0
2	21.0	18.5	16.0	45 × 45	37 × 36	30 × 32	4.8
3	22.5	22.0	21.0	55 × 53	47 × 46	41 × 43	2.4
4	23.0	22.5	22.0	54 × 55	53 × 54	50 × 49	2.0
5	19.0	17.0	15.5	42 × 40	37 × 38	31 × 32	4.7
6	23.5	22.0	20.5	56 × 58	50 × 50	39 × 40	3.3
7	24.5	24.0	23.5	58 × 63	57 × 56	55 × 55	2.1
8	24.0	24.0	23.5	63 × 62	60 × 61	59 × 58	1.6

Table 4
Mechanical properties of concrete

Mix no.	Compressive strength (MPa)				Modulus of elasticity (GPa)			
	1 day	3 days	7 days	28 days	1 day	3 days	7 days	28 days
1	9.6	20.3	25.3	31.1	14.0	21.0	24.9	26.9
2	21.8	37.7	43.0	47.1	22.1	29.4	31.2	32.9
3	25.0	42.8	49.4	55.5	24.9	30.1	33.2	34.3
4	30.3	48.1	58.2	66.2	25.2	32.5	35.7	36.2
5	6.1	16.1	20.7	29.3	12.3	18.0	19.5	26.7
6	14.0	29.3	37.4	45.9	16.6	25.9	28.4	32.4
7	14.2	35.0	40.7	52.6	18.1	27.3	29.0	33.6
8	13.4	38.9	45.6	62.4	16.4	28.5	32.4	34.5

Table 4 shows the compressive strength and modulus of elasticity for the eight concretes at 1, 3, 7 and 28 days as measured in accordance with ASTM C39 and C469, respectively. The compressive strength at 28 days ranged from 29.3 to 66.2 MPa, and the corresponding modulus of elasticity ranged from 26.7 to 36.2 GPa. In general, each of FA concretes exhibited lower strength and lower modulus of elasticity than the corresponding OPC concretes with the same w/cm at a given age.

3.2. Measurement of UPV and waveform analysis

Fig. 2 shows typical ultrasonic waveforms for mortar with w/cm = 0.50 obtained at three different ages by recording the voltage signal at the receiving transducer using an oscilloscope. Use of an oscilloscope was necessary to observe these waveforms because the commercial UPV measurement device only provided numerical values of UPV or the transit time of ultrasonic pulse. The downward arrow in each plot indicates the instant when the input pulse was transmitted. The upward arrow indicates the instant when the ultrasonic wave was considered to have reached the receiving transducer. The time duration between these two arrows is given as Δt in the inset of each plot. By subtracting the transit time of the ultrasonic pulse through the short acrylic paths from Δt, t_p in Eq. (1) was obtained, and the UPV was calculated from Eq. (1).

Comparison of Fig. 2a–c demonstrates that the transit time of the ultrasonic pulse decreased with age, meaning a steady increase of UPV with age. Note in Fig. 2 that the dominant frequency component in the waveform varies with age. The power spectra of these waveforms were obtained by conducting a fast Fourier transform (FFT) analysis and are shown in Fig. 3. Fig. 3a–c, respectively, indicate that the dominant frequency was close to the center frequency (e.g., 53 kHz) of the transducers at very early ages up to 8 h, then shifted to much lower values (e.g., 2–10 kHz) at intermediate ages between 8 and 12 h and finally returned to the

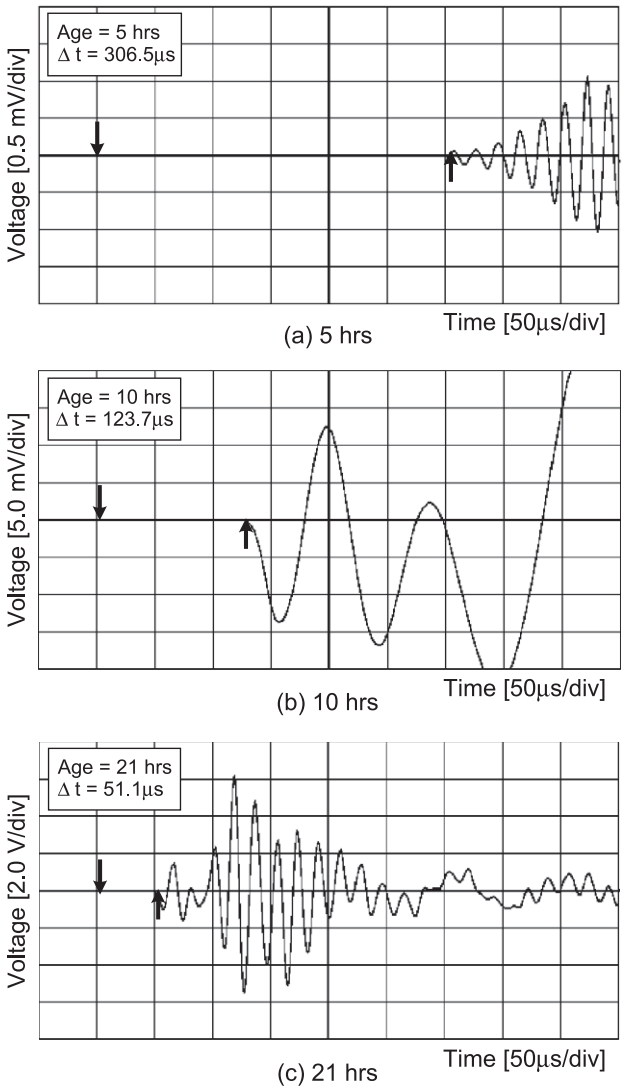

Fig. 2. Ultrasonic waveforms obtained using oscilloscope for mortar with w/cm = 0.50.

vicinity of the transducers' center frequency (e.g., 55 kHz) after 12 h of age.

This interesting frequency-domain phenomenon may be explained as follows. At very early ages (Figs. 2a and 3a), the specimen may be considered as viscous suspension through which no frequency component of ultrasonic wave easily propagates (note the very small ordinate magnitudes of Figs. 2a and 3a). This situation corresponds to the very early age when only longitudinal waves, no shear waves, can propagate [12,13]. In this situation, the transducers' center frequency component appears relatively dominant among all suppressed frequency components. As the hydration process continues (Figs. 2b and 3b), the specimen changes from viscous suspension into water-saturated porous solid with nonvanishing elastic moduli [19–21]. Thus, low-frequency components now begin to propagate with increased ease through the gradually forming porous solid path before the high-frequency components do, as may be observed in Fig. 3b. This is in agreement with previous studies [13,18,20]. Note also that the ordinate magnitudes of Figs. 2b and 3b are much greater than those of Figs. 2a and 3a, respectively, which means much more significant wave transmission through the specimen. As the hydration continues further (Figs. 2c and 3c), the porous solid structure becomes more established, allowing for even easier transmission of all frequency components, resulting in even greater ordinate magnitudes. Then, the transducers' frequency components appear relatively dominant again, among all the frequency components now activated (see Fig. 3c).

3.3. Evolution of UPV

Fig. 4 shows the evolution of the UPV during the first 24 h for all mortars (hollow marks in the figures) and concretes (solid marks). In the figure, the vertical solid and dashed lines indicate the initial and final setting times of mortars as found using the penetration resistance test method, respectively.

It can clearly be seen from Fig. 4 that the UPV of concrete was at very early ages similar to that of mortar with the same w/cm but developed relatively earlier and became relatively greater afterwards. Further discussion in this regard will be given in Section 3.4. The same trend may also be observed with the OPC mortar series as compared with the corresponding FA mortar series with same w/cm.

Furthermore, it may be noted from Fig. 4 that the initial and final setting times of high-performance mortars are longer than those of the normal-strength mortar in the same series of OPC or FA. This setting retardation of high-performance mortars is thought to result from the use of

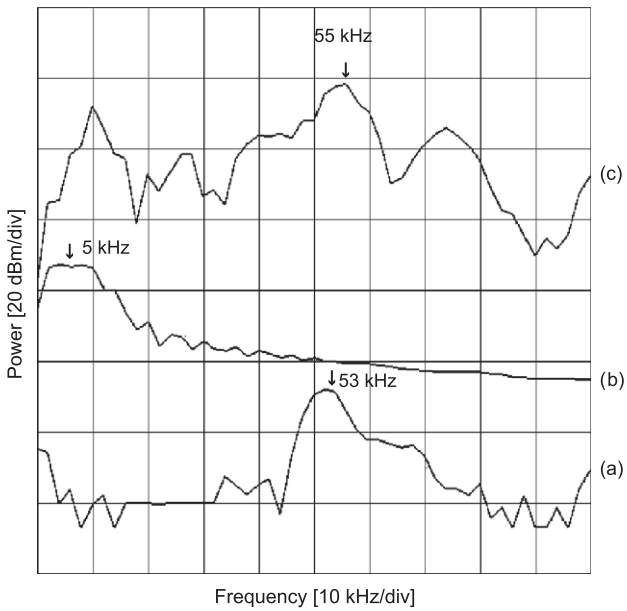

Fig. 3. Evolution of frequency spectra of waveforms in Fig. 2: (a) 5, (b) 10 and (c) 21 h.

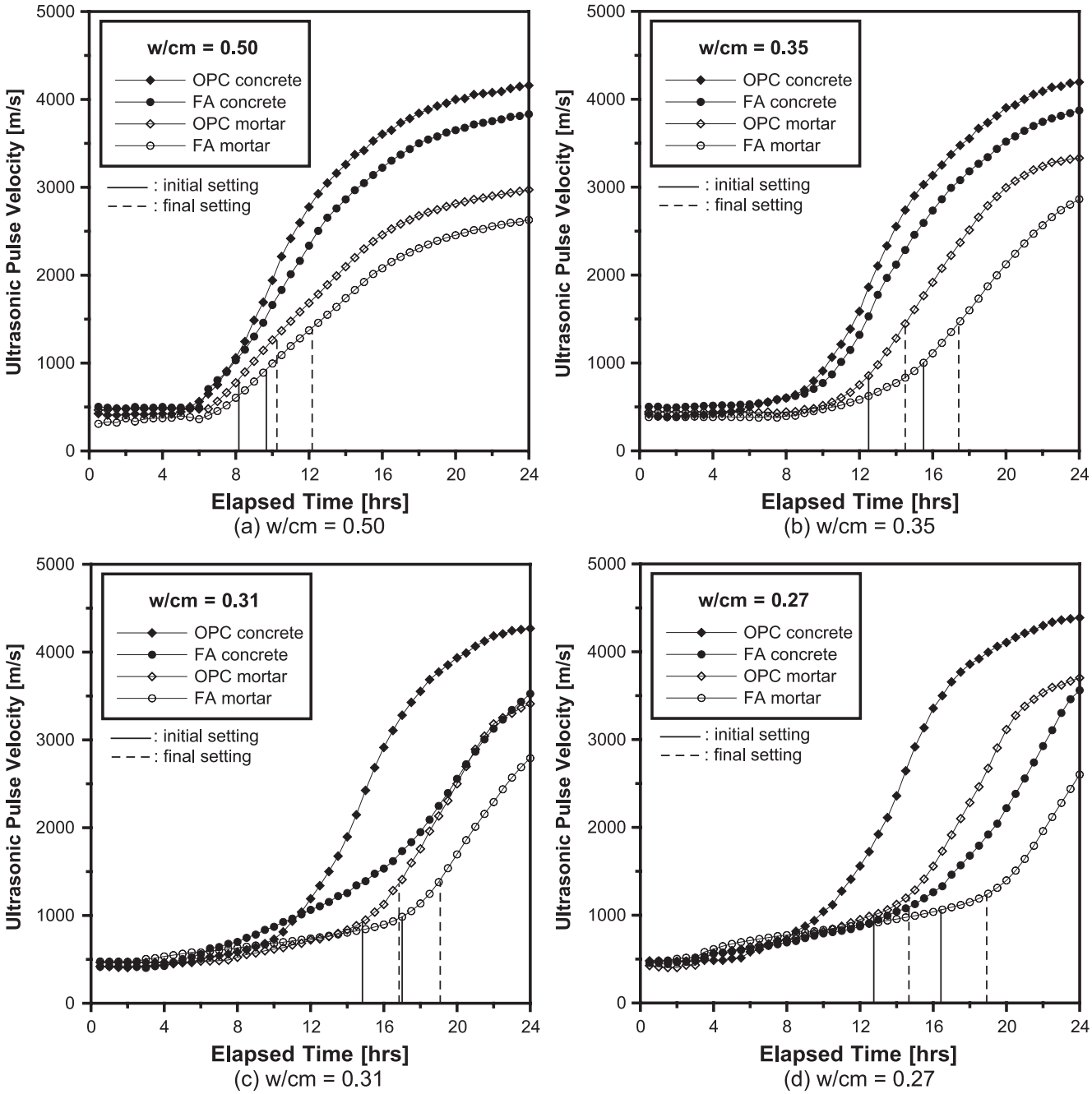

Fig. 4. Evolution of UPV of mortar and concrete specimens with various w/cm.

HRWR having retardation effect and may thus depend on the type and dosage of HRWR used.

3.4. Discussions on evolution of UPV

All UPV curves in Fig. 4 are similar to the curve in Fig. 5 as observed by other researchers [4–14]. Fig. 5 divides the UPV evolution behavior into three steps, Steps 1–3 [8,9,14]. During Step 1, hydrates begin to form after the dormant induction period. In Step 1, ultrasonic waves propagate through the water-like viscous suspension. As the hydration continues, the increased tortuosity of the pore or air-filled space due to the formation of hydration products often causes slightly decreasing UPV in Step 1 [4,5,12,14]. When the minimum quantity of hydration products required for a sharp climb of UPV is achieved, Step 2 begins. According to Boumiz et al. [14], more and more cement grains continue to become connected in Step 2, and the percolation of solid phase seems to occur in the early part of Step 2, after which shear waves can propagate [13,20]. In Step 2, the water-saturated porous solid structure becomes more and more connected as newly formed

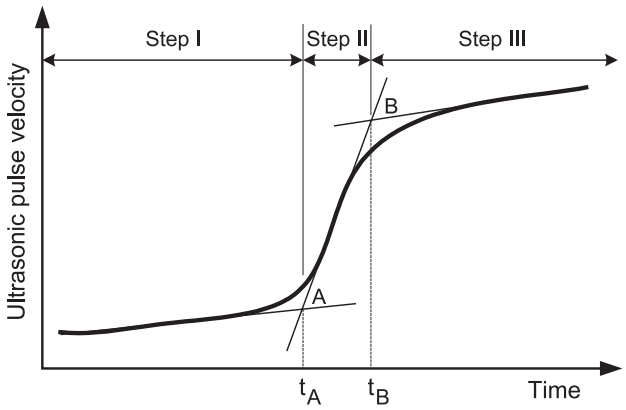

Fig. 5. Schematic representation of typical evolution of UPV.

hydration products fill in the pores; thus, the UPV increases. As the volume of pores is decreased by filling of hydration products, the UPV levels off and approaches its asymptotic value in the solid structure.

As briefly mentioned in Section 3.3, an analysis of Fig. 4 reveals that the UPVs of all concrete mixtures at very early ages are about equal to but at later ages are much greater than those of the corresponding mortar mixtures having the same w/cm. These close UPV values of concrete and mortar at very early ages may be explained by the above description of Step 1 in Fig. 5: ultrasonic waves at these very early ages propagate mainly through the common water-like viscous phase, thus unaffected by the presence of coarse aggregates. The very low initial UPVs in the 300–500 m/s range may be explained either by the highly elongated length of wave path because of the suspended cement grains in fresh mortar [16] or by the effects of the entrapped air [4,5,12]. Another possible explanation is the incomplete mixing of specimen having low w/cm, resulting in insufficient coupling of cement particles with water [18]. At later ages (Steps 2 and 3), however, the UPV of concrete becomes greater than that of corresponding mortar. This may be because ultrasonic waves in these steps propagate mainly through the solid phase structure and because the coarse aggregates exclusively contained in the concrete specimens have higher stiffness than the constituents of mortars.

Note also in Fig. 4 that the UPVs of OPC concrete and mortar mixtures are at very early ages similar to but are at later ages greater than those of the corresponding FA mixtures with the same w/cm. This very early-age behavior may again be accounted for by waves propagating through the common phase of viscous suspension. The later-age behavior is because replacing cement by FA retards the hydration reaction as observed by the simulation of a three-dimensional model [19]; thus, the setting retardation of FA mortars may depend on the FA content.

Furthermore, comparisons of Fig. 4a–d reveal that the UPV development profiles for high-performance mixtures are different from those of normal-strength mixtures. Note in Fig. 4a for normal-strength mixtures that the UPVs remained essentially constant in Step 1 but abruptly increased in Step 2. This, however, is not the case for high-performance mixtures (see Fig. 4b–d), which exhibited slow, gradual and prolonged development of UPV in Step 1 and smooth transition to Step 2. This trend of high-performance mixtures has not been observed previously in the literature; furthermore, it is rather contrary to the often reported slight decrease of UPV in Step 1 [4,5,12,14]. The cause of this early and prolonged increase of UPV with low w/cm is not clear at this point, but a reasonable explanation is that the cement particles in the low w/cm cases may begin to become connected at relatively early ages because of the relatively short distances between them, but massive hydration is delayed due to the HRWR. This delay of massive hydration is more significant in FA series than in OPC series (see Fig. 4), which is due to the presence of the FA in addition to the HRWR effects.

3.5. Specification of characteristic UPV values

As mentioned in Section 1, researchers have suggested several methods for identifying characteristic times in the hydration of cements from ultrasonic measurements. Two of them are relevant to the present work and are thus considered here. According to Chotard et al. [8] and Garnier et al. [10], the transition points between adjacent steps in Fig. 5 may be expected to correspond to distinct microstructural changes of the specimen. These transition points may be determined as the intersections of three straight lines tangent to the curve (e.g., Points A and B in Fig. 5). This method is particularly useful for high-performance mixtures, where the UPV curve does not show abrupt development at the beginning of Step 2, unlike normal-strength mixtures, as discussed in Section 3.4 concerning Fig. 4b–d. Point A may be regarded as a criterion for the initial formation of the porous solid phase, which will be called Criterion 2 in this paper. (The initial and final setting times according to ASTM C403 will be called Criteria 1I and 1F, respectively).

The second approach is associated with the increasing rate of wave velocity. In the manner similar to Kakuta and Kojima [6], another characteristic time in the setting process may be designated as the instant when the increasing rate of wave velocity reaches its maximum. At this particular instant (in Step 2 of Fig. 5), the increase rate of effective stiffness will reach its maximum, after which the formation rate of the porous solid structure will decline. This point of the maximum UPV development may be found from a polynomial fitted to the UPV curve in Step 2, and this criterion will be called Criterion 3 in this paper.

Figs. 6 and 7 show the UPV values for mortars and concretes, respectively, that correspond to the characteristic points in the UPV evolution according to the four different criteria defined above. According to Criterion 1I, UPVs at the initial setting of OPC mortars and concretes are slightly lower than those of corresponding FA mortars and concretes. This is due to the retarded setting of FA mixtures (see

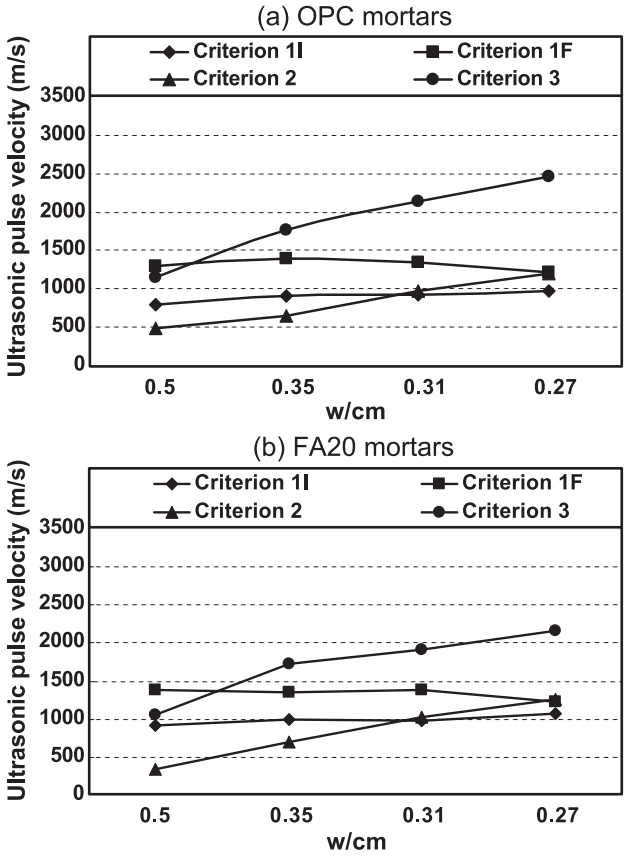

Fig. 6. Variation of characteristic UPV for setting of mortar.

Fig. 4), which allowed the UPV of each FA mixture to develop above that of the corresponding OPC. Furthermore, it may be observed from Fig. 6 that the UPVs under Criterion 1I slightly increases with decreasing w/cm in both OPC and FA mortars. It is observed from Fig. 6 that the UPV at the initial setting lied within a relatively narrow range, 800–980 m/s for OPC mortars and 920–1070 m/s for FA mortars. Although these UPV values themselves may be considered as artifacts because of the variable effects from the variable type and dosage of HRWR, the approximate ranges of UPV given above for OPC and FA mortars may still be of good practical value in the actual use of HPC if UPV is to be used as a parameter equivalent to the penetration resistance. Unlike mortars, the UPV of concretes shows neither such monotonous increases with decreasing w/cm nor such narrow ranges as may be seen from Fig. 7. These different behaviors of mortars and concretes cannot clearly be accounted for now, but they seem to support the argument that Criterion 1I does not represent the inherent changes occurring in the hydrating specimens.

Similar examination of UPVs according to Criterion 1F reveals that the UPVs of mortar mixtures at the final setting were within narrow ranges when compared with those of concrete mixtures. As in Criterion 1I, UPVs of mortars exhibited a monotonous trend with varying w/cm whereas those of concretes did not (compare Figs. 6 and 7).

On the other hand, it may be observed from Figs. 6 and 7 that UPVs of both mortars and concretes (with or without FA) in Criteria 2 and 3, in general, increased as the w/cm decreased. This consistent tendency, unlike in the cases of Criteria 1I and 1F, reinforces the claim that Criteria 2 and 3 better reflect the microstructural changes in the specimens. In particular, the increase of UPV with decreasing w/cm in Criterion 2 may be accounted for by the following graphical interpretation. As the w/cm decreases, the initial slopes (i.e., those of Step 1 in Fig. 5) tend to increase as may be seen by comparing Fig. 4a with Fig. 4b–d and thus yield higher UPV in Criterion 2. Recall that this tendency of initial slope increase with decreasing w/cm may be attributed to the relatively short distances between cement particles, which is an inherent characteristic of high-performance mixtures. Therefore, the consistent tendency of increasing UPV with decreasing w/cm in Criterion 2 may be considered to represent an inherent characteristic of the cement setting process.

Another important observation from Figs. 6 and 7 is that the UPVs in Criterion 2 at each w/cm value do not vary much among the four combinations: mortar and concrete with and without FA. The graphical explanation for this is that the ordinate of the intersection point A in Fig. 5 is not much affected by a postponed Step 2 curve (as observed in the FA series when compared with OPC series and in the

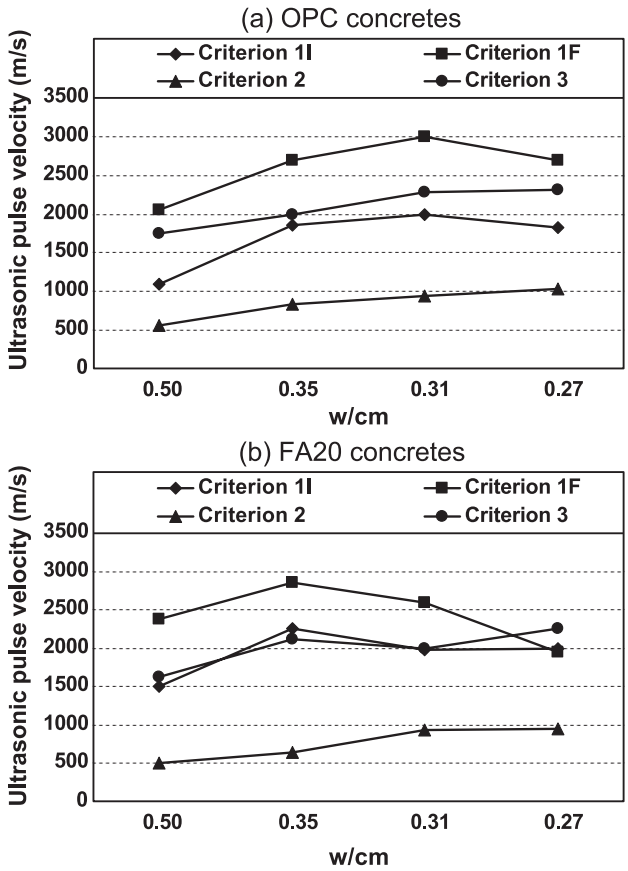

Fig. 7. Variation of characteristic UPV for setting of concrete.

mortars when compared with concretes in Fig. 4) as long as the slope of Step 1 is fixed and is not great as in Fig. 4. This point is of practical value because a target value of UPV in Criterion 2 thus might be specified at a given w/cm as a constant or within a very narrow range that is valid for both concrete and mortar with or without FA.

Further, the UPV ranges for concrete in both Criteria 2 and 3, particularly the latter, are observed in Figs. 6 and 7 to be smaller than the corresponding ranges for mortar. This observation seems to imply that once the solid phase begins to form, coarse aggregates have dominant effects on the UPV development, resulting in relatively less effects on the UPV of other factors such as w/cm.

For practical applications, setting times must be determined directly on the concrete mixture particularly because mortar specimens for the penetration resistance test can hardly be obtained from HPC. In this respect, the UPV monitoring system used in this study is very effective. Extensive in-depth studies, however, need to be conducted to determine the setting criteria for concrete as well as mortar as a function of w/cm.

4. Conclusions

The following conclusions may be drawn from this study.

(1) An ultrasonic monitoring system has been used to successfully measure the UPV of both mortar and concrete beginning immediately after mixing. This method demonstrated a great practical advantage to the conventional method of penetration resistance because it could be conducted directly on concrete rather than on sieved mortar. This is particularly useful for HPC from which mortar samples can hardly be obtained because of its high viscosity.

(2) The UPV development curves of all specimens resembled a curve that consists of three steps. At very early ages in Step 1, the UPVs of all concrete and mortar mixtures with the same w/cm were almost the same regardless of the presence of coarse aggregates or FA. This was explained based on the hypothesis that ultrasonic waves propagate through the phase of viscous suspension, which is initially common among all specimens. The UPV profiles at later ages (Steps 2 and 3) differed from each other: UPVs of concrete mixtures were greater than those of mortar mixtures and those of OPC series were greater than those of FA series. These features were respectively explained by the higher stiffness of coarse aggregates and the retarding effects of FA.

(3) The initial slope of the UPV evolution curve (i.e., the slope of Step 1) was observed to increase with decreasing w/cm in contrast to the zero slope for a high w/cm case considered. This was explained by the relatively shorter distances between cement particles in cases of low w/cm and thus increased chances of their being connected at earlier times.

(4) The UPVs corresponding to the initial and final setting, identified through the method of penetration resistance, were examined for various mortar mixtures. As a result, certain ranges of UPV with reasonable widths were suggested for the initial setting times: i.e., 800–980 and 920–1070 m/s for the initial setting of OPC and FA mortar series, respectively. The UPVs corresponding to the initial setting increased with decreasing w/cm in mortar specimens but did not show a monotonous tendency in concrete specimens. The same was true of the UPVs corresponding to the final setting.

(5) Two alternative methods for characterizing the setting process were considered that identify particular points in the UPV development curves (i.e., the instant when the UPV begins to develop and the instant when the UPV development rate is maximum). These two alternative methods seem to better reflect the microstructural changes of mortar mixtures than the method of penetration resistance because of the consistent tendency of increasing UPV with decreasing w/cm in both mortars and concretes (with and without FA). It was also found that the UPV at the beginning of its development does not vary much among the four combinations having the same w/cm value: mortar and concrete with and without FA. This demonstrates that further development of this method might provide a generally valid target UPV or a narrow range of UPV to designate the setting for each value of w/cm.

Acknowledgements

The authors acknowledge the financial support of SAFE Research Center sponsored by Korea Science and Engineering Foundation (KOSEF).

References

[1] Standard test method for time of setting of concrete mixtures by penetration resistance, ASTM C 403, Annual Books of ASTM Standards, ASTM, Philadelphia, USA (1985) 273–276.
[2] P.K. Mehta, J.M. Monteiro, Concrete: Structure, Properties, and Materials, 2nd ed., Prentice-Hall, New Jersey, 1993.
[3] S.P. Pessiki, N.J. Carino, Setting time and strength of concrete using the impact-echo method, ACI Mater. J. 85 (1988) 389–399.
[4] J. Keating, D.J. Hannant, A.P. Hibbert, Comparison of shear modulus and pulse velocity techniques to measure the build-up of structure in fresh cement pastes used in oil well cementing, Cem. Concr. Res. 19 (1989) 554–566.
[5] J. Keating, D.J. Hannant, A.P. Hibbert, Correlation between cube strength, ultrasonic pulse velocity and volume change for oil well cement slurries, Cem. Concr. Res. 19 (1989) 715–726.
[6] S. Kakuta, T. Kojima, Evaluation of very early age concrete using a wave propagation method, in: L. Taerwe, H. Lambotte (Eds.), Quality

Control of Concrete Structures, E&FN SPON, Ghent, Belgium, 1991, pp. 163–172.
[7] S. Popovics, R. Silva-Rodriguez, J.S. Popovics, V. Martucci, Behavior of ultrasonic pulses in fresh concrete, New Experimental Techniques for Evaluating Concrete Materials and Structural Performance, SP-143, ACI, Detroit, MI, USA (1993) 207–225.
[8] T. Chotard, N. Gimet-Brert, A. Smith, D. Fargeto, J.P. Bonnet, C. Gault, Application of ultrasonic testing to describe the hydration of calcium aluminate cement at the early age, Cem. Concr. Res. 31 (2001) 405–412.
[9] A. Smith, T. Chotard, N. Gimet-Breart, D. Fargeot, Correlation between hydration mechanism and ultrasonic measurements in an aluminous cement: effect of setting time and temperature on the early hydration, J. Eur. Ceram. Soc. 22 (2002) 1947–1958.
[10] V. Garnier, G. Corneloup, J.M. Sprauel, J.C. Perfumo, Setting time study of roller compacted concrete by spectral analysis of transmitted ultrasonic signals, NDT&E Intl. 28 (1) (1995) 15–22.
[11] H.W. Reinhardt, C.U. Grosse, A.T. Herb, Ultrasonic monitoring of setting and hardening of cement mortar, Mater. Struct. 33 (2000) 580–583.
[12] C.M. Sayers, R.L. Grenfell, Ultrasonic propagation through hydrating cements, Ultrasonics 31 (1993) 147–153.
[13] R. D'Angelo, T.J. Plona, L.M. Schwartz, P. Coveney, Ultrasonic measurements on hydrating cement slurries: onset of shear wave propagation, Adv. Cem. Based Mater. 2 (1995) 8–14.
[14] A. Boumiz, C. Vernet, F. Cohen Tenoudji, Mechanical properties of cement pastes and mortars at early ages, Adv. Cem. Based Mater. 3 (1996) 94–106.
[15] M.A. Biot, Theory of propagation of elastic waves in a fluid-saturated porous solid, J. Acoust. Soc. Am. 28 (1956) 168–191.
[16] J.R. Rapoport, J.S. Popovics, V.K. Subramaniam, S.P. Shah, Using ultrasound to monitor stiffening process of concrete with admixtures, ACI Mater. J. 97 (2000) 675–683.
[17] M.I. Valic, Hydration of cementitious materials by pulse echo USWR method, apparatus and application examples, Cem. Concr. Res. 30 (2000) 1633–1640.
[18] A. Feylessoufi, F. Cohen Tenoudji, V. Morin, P. Richard, Early ages shrinkage mechanisms of ultra-high-performance cement-based materials, Cem. Concr. Res. 31 (2001) 1573–1579.
[19] D.P. Bentz, E.J. Garboczi, Percolation of phases in a three-dimensional cement paste microstructural model, Cem. Concr. Res. 21 (1991) 325–344.
[20] D.P. Bentz, P.V. Coveney, E.J. Garboczi, M.F. Kleyn, P.E. Stutzman, Cellular automaton simulations of cement hydration and microstructure development, Modell. Simul. Mater. Sci. Eng. 2 (1994) 783–808.
[21] D.P. Bentz, Three-dimensional computer simulation of Portland cement hydration and microstructure development, J. Am. Ceram. Soc. 80 (1) (1997) 3–21.